Free Radical Biology and Medicine 90 (2016) 206–218

Contents lists available at ScienceDirect

Free Radical Biology and Medicine

journal homepage: www.elsevier.com/locate/freeradbiomed

Original Contribution

HERPUD1 protects against oxidative stress-induced apoptosis through downregulation of the inositol 1,4,5-trisphosphate receptor

Felipe Paredes [a], Valentina Parra [a], Natalia Torrealba [a], Mario Navarro-Marquez [a], Damian Gatica [a], Roberto Bravo-Sagua [a], Rodrigo Troncoso [a,b], Christian Pennanen [a], Clara Quiroga [c], Mario Chiong [a], Christa Caesar [d], W. Robert Taylor [d,e], Jordi Molgó [f], Alejandra San Martin [e], Enrique Jaimovich [g], Sergio Lavandero [a,g,h,*]

[a] Advanced Center for Chronic Diseases (ACCDiS), Facultad de Ciencias Químicas y Farmacéuticas & Facultad de Medicina, Universidad de Chile, 838049 Santiago, Chile
[b] Instituto de Nutrición y Tecnología de los Alimentos (INTA), Universidad de Chile, Santiago, Chile
[c] ACCDiS, Cardiovascular Diseases Division, Faculty of Medicine, Pontifical Catholic University of Chile, Santiago, Chile
[d] Wallace H. Coulter Department of Biomedical Engineering, Georgia Institute of Technology/Emory University, Atlanta, GA, USA
[e] Department of Medicine, Division of Cardiology, Emory University School of Medicine, Atlanta, GA, USA
[f] Institut des Neurosciences Paris-Saclay, UMR 9197, 91190 Gif sur Yvette, France
[g] Centro de Estudios Moleculares de la Célula, Facultad de Medicina, Universidad de Chile, Santiago, Chile
[h] Department of Internal Medicine (Cardiology Division), University of Texas Southwestern Medical Center, Dallas, TX, USA

ARTICLE INFO

Article history:
Received 9 May 2015
Received in revised form
17 November 2015
Accepted 20 November 2015
Available online 23 November 2015

Keywords:
HERPUD1
Oxidative stress
IP3 receptor
Cell death

ABSTRACT

Homocysteine-inducible, endoplasmic reticulum (ER) stress-inducible, ubiquitin-like domain member 1 (HERPUD1), an ER resident protein, is upregulated in response to ER stress and Ca^{2+} homeostasis deregulation. HERPUD1 exerts cytoprotective effects in various models, but its role during oxidative insult remains unknown. The aim of this study was to investigate whether HERPUD1 contributes to cytoprotection in response to redox stress and participates in mediating stress-dependent signaling pathways. Our data showed that HERPUD1 protein levels increased in HeLa cells treated for 30 min with H_2O_2 or angiotensin II and in aortic tissue isolated from mice treated with angiotensin II for 3 weeks. Cell death was higher in *HERPUD1* knockdown (sh-*HERPUD1*) HeLa cells treated with H_2O_2 in comparison with control (sh-*Luc*) HeLa cells. This effect was abolished by the intracellular Ca^{2+} chelating agent BAPTA-AM or the inositol 1,4,5-trisphosphate receptor (ITPR) antagonist xestospongin B, suggesting that the response to H_2O_2 was dependent on intracellular Ca^{2+} stores and the ITPR. Ca^{2+} kinetics showed that sh-*HERPUD1* HeLa cells exhibited greater and more sustained cytosolic and mitochondrial Ca^{2+} increases than sh-*Luc* HeLa cells. This higher sensitivity of sh-*HERPUD1* HeLa cells to H_2O_2 was prevented with the mitochondrial permeability transition pore inhibitor cyclosporine A. We concluded that the HERPUD1-mediated cytoprotective effect against oxidative stress depends on the ITPR and Ca^{2+} transfer from the ER to mitochondria.

1. Introduction

Reactive oxygen species (ROS) participate in host defense, gene expression, cell growth and inflammation [1]. At mild concentrations, ROS exert regulatory functions through oxidation of redox sensors. Excessive or deregulated ROS production (termed oxidative stress) may cause direct damage to proteins, lipids and DNA, contributing to the onset of several diseases [1–3]. In the cardiovascular system, this double-edged behavior mediates the pathophysiological actions of angiotensin II (Ang II), the primary effector of the renin–angiotensin system. In vascular smooth muscle cells (VSMCs), this peptide induces contraction, migration and proliferation through ROS signaling [4–6]. Indeed, Ang II-induced

Abbreviations: ActD, actinomycin D; Ang II, angiotensin II; Cat, catalase; CHX, cycloheximide; CsA, cyclosporine A; Cyt-C, cytochrome c; ER, endoplasmic reticulum; ERAD, ER-associated degradation; ERE, ER stress; HERPUD1, homocysteine-induced ER protein; ITPR, inositol 1,4,5-trisphosphate receptor; JNK, c-Jun N-terminal kinase; MPP^+, methylphenylpyridinium; MPTP, mitochondrial permeability transition pore; Nox, NAD(P)H oxidase; RYR, ryanodine receptor; VSMC, vascular smooth muscle cells; XeB, xestospongin B

* Corresponding autor at: Advanced Center for Chronic Disease (ACCDiS), Facultad de Ciencias Químicas y Farmacéuticas & Facultad Medicina, Universidad de Chile, 838049 Santiago, Chile.
E-mail address: slavander@uchile.cl (S. Lavandero).

http://dx.doi.org/10.1016/j.freeradbiomed.2015.11.024
0891-5849/

cardiac hypertrophy can be inhibited by antioxidants [7–9] or through overexpression of catalase (Cat), which catalyzes hydrogen peroxide (H_2O_2) decomposition [10–12].

One of the most abundant and stable ROS is H_2O_2 [13], which can trigger cell death programs such as apoptosis and necrosis [3]. Elevated ROS levels cause influx of Ca^{2+} into the cytoplasm, increasing oxidative stress [14]. Additionally, alterations in the redox environment of the endoplasmic reticulum (ER), the main storage site for intracellular Ca^{2+}, results in the release of Ca^{2+} from the ER [15]. Both oxidative stress and high cytoplasmic Ca^{2+} levels can result in cytotoxicity by the activation of the apoptotic cell death program [16,17]. Ultimately, it has shown that cytoplasmic Ca^{2+} overload can result in cytotoxicity, concomitant with activation of the intrinsic, or mitochondria-dependent, apoptotic pathway [18]. Consequently, mitochondrial Ca^{2+} overload triggers the opening of the mitochondrial permeability transition pore (MPTP), thereby committing to cellular demise [19,20].

ER plays a pivotal role in both cell susceptibility and survival. Perturbations in ER homeostasis (termed ER stress) induce several compensatory responses that may revert the cell death decision. Homocysteine-induced ER stress-inducible, ubiquitin-like domain member 1 (HERPUD1), also known as Herp, is a 54 kDa transmembrane protein whose levels increase acutely in response to ER stress [21]. Agents that alter ER proteostasis (e.g. tunicamycin, 2-mercaptoethanol and homocysteine), as well as others that deplete ER Ca^{2+} stores (e.g. A23187 and thapsigargin), also induce ER stress [21]. While HERPUD1 has no enzymatic activity or a defined biological function, this ER protein has shown to regulate ER-associated degradation (ERAD) by interacting with proteins involved in retrotranslocation, ubiquitination and degradation of misfolded proteins [22,23]. HERPUD1 has cytoprotective roles against ER stress, as it decreases the activity of various caspases, prevents mitochondrial potential collapse and diminishes c-Jun N-terminal kinase (JNK) activation [24–26]. Moreover, our group has recently shown that HERPUD1 acts as a negative regulator of autophagy by inducing the proteasomal degradation of Beclin-1 [27]. These results show that HERPUD1 not only regulates ERAD and cytoprotection, but also acts as an important regulator of protein degradation and stress responses.

HERPUD1 forms complexes with the inositol 1,4,5-trisphosphate receptor (ITPR) and the ryanodine receptor (RYR), the most prominent Ca^{2+} channels in the ER membrane. This interaction leads to ITPR and RYR proteasome-dependent degradation, thus allowing HERPUD1 to directly regulate ER Ca^{2+} release [28]. HERPUD1 over-expression in PC12 cells consistently decreases Ca^{2+} output after bradykinin or thapsigargin treatment, while HERPUD1 silencing has the opposite effect [24]. Importantly, HERPUD1 over-expression attenuates the mitochondrial Ca^{2+} increase induced by methylphenylpyridinium (MPP^+), suggesting that HERPUD1 may inhibit Ca^{2+} transfer between the ER and mitochondria [29]. Despite this evidence, it remains unknown whether HERPUD1 exerts its protective effect against oxidative stress by regulating the ITPR and Ca^{2+} signaling.

Here, we investigate the role of HERPUD1 in H_2O_2-induced cell death. We show that HERPUD1 protein levels increased in HeLa cells treated for 30 min with H_2O_2 or Ang II. Moreover, *HERPUD1* mRNA increased in total aortic tissue isolated from mice treated with Ang II for 3 weeks. H_2O_2 stimulated higher increases in cytosolic and mitochondrial Ca^{2+} in sh-*HERPUD1* HeLa cells compared with sh-*Luc* HeLa cells. Cell death was also higher in sh-*HERPUD1* HeLa cells treated with H_2O_2. This effect on cell viability was prevented with BAPTA-AM or ITPR antagonist xestospongin B (XeB), suggesting that the HERPUD1-dependent cytoprotective effect against oxidative stress is regulated by the ITPR and the influx of Ca^{2+} from the ER to mitochondria.

2. Materials and methods

2.1. Antibodies and reagents

Dulbecco's modified Eagle medium (DMEM), Earle's Balanced Salt Solution medium, propidium iodide, Triton X-100, EGTA, cyclosporine A, angiotensin II, carboxy-cyanide-3-chlorophenylhydrazone (CCCP), actinomycin D (ActD), cycloheximide (CHX), histamine, cytochalasin B, Triton X-100, catalase (C-1345), anti-ACTB (β-actin) and anti-TUBB (β-tubulin) antibodies were from Sigma-Aldrich Co. (St. Louis, MO). Secondary anti-mouse and rabbit antibodies and 4EGI were from Calbiochem (Burlington, Canada). Fetal Bovine Serum (FBS), Opti-MEM, trypsin, L-glutamine, non-essential amino acids, HEPES, EDTA, puromycin and penicillin/streptomycin were from GIBCO (Paisley, Scotland, UK). Mitotracker green-FM, tetramethylrhodamine methyl ester perchlorate, Fluo-4AM, Fura-2AM, Rhod-FF, 2′,7′-dichlorodihydrofluorescein diacetate (H_2DCFDA), BAPTA-AM, lipofectamine 2000, oligofectamine and Alexa Fluor 488 and 568 antibodies were from Invitrogen (Molecular Probes-Invitrogen, Carlsbad, CA). Anti-HERPUD1 (Herp) was from BIOMOL Research Laboratories (Plymouth Meeting, PA) and Anti-ITPR was from ABR (Thermo Fischer Scientific (Rockford, IL)). Thapsigargin was obtained from Enzo Life Sciences, Inc (Farmingdale, NY). All materials for SDS-PAGE, nitrocellulose and PVDF membranes were from Bio-Rad Laboratories (Hercules, CA). Fluorescence mounting medium was from DAKO Corporation (CA). Organic and inorganic compounds, acids, H_2O_2 and solvents were from Merck (Darmstadt, Germany). SuperSignal West Pico chemiluminescent substrate was from Pierce (Rockford, IL). Xestospongin B was isolated and produced in the Laboratory of Prof. Jordi Molgó (Institut de Neurobiologie Alfred Fessard, Gif-sur-Yvette, France) and used as previously described [30].

2.2. Cell culture, siRNA transfection and production of stable knockdown cells

HeLa cells and MEFs were cultured in DMEM supplemented with 10% FBS and 100 units/mL penicillin G sodium and 100 μg/mL streptomycin sulfate at 37 °C under 5% CO_2. MEF cells were supplemented with 5 mM L-glutamine and 10 mM HEPES buffer. To generate a stable cell line that express the sh-*Luc* or sh-*HERPUD1*, HeLa cells were transfected in Opti-MEM medium with Lipofectamine 2000 according to manufacturer instructions, using the following plasmids: VSV-G, pMDL, REV and PLKO1-sh-*HERPUD1* or PLKO1-sh-*Luc* (kindly donated by Dr. H. Komano, National Institute for Longevity Sciences, Obu, Aichi, Japan). After 48 h, the conditioned medium with lentiviral particles was collected and filtered with 0.45-μm pore diameter filters. After 48 h of viral transduction, medium-containing puromycin (2 μg/mL) was used for selecting sh-*HERPUD1* and sh-*Luc* cells. Using this strategy we knocked down HERPUD1 levels from 1.0 ± 0.04 to 0.4 ± 0.02 in HeLa cells (Fig. S1A). This data was also corroborated overexpressing a mouse (PGI3-m*HERPUD1*) and a human (PGI3-h*HERPUD1)* form of the protein in the knocked down cells. Only the mouse form of the protein was able to rescue the HERPUD1 protein levels in the sh-*HERPUD1* cell line (Fig. S1A).

Additionally, HeLa cells were transfected with 100 nM of a control siRNA, two siRNA against HERPUD1 (si-*HERPUD1* 1 and 2 [Sigma-Aldrich Co, St. Louis, MO]) or a plasmid to overexpress the human HERPUD1 protein (PGI3-h*HERPUD1*, OriGene), together with Lipofectamine 2000 (Invitrogen, 11668-019) in Opti-MEM medium (GIBCO, 31985-070) overnight according to manufacturer instructions. In the case of the siRNA's, two different were used, obtaining the best results with the one that arbitrarily we called siRNA number 2 (si-*HERPUD1* 2) (Fig. S1C). The use of this siRNA corroborated all the main results obtained with the sh-*HERPUD1*

cell line (Fig. S2D–G).

2.3. Animal model

Wild-type and Cat transgenic-overexpressing mice were treated with Ang II (Sigma-Aldrich A6402) reconstituted in saline, infused via an Alzet mini-osmotic pump at a dose of 0.75 mg/kg/day for 7 days [31]. Ang II treated wild type animals increased blood pressure from 103 ± 11 to 164 ± 28 mmHg, while in Ang II treated Cat transgenic-overexpressing mice increased blood pressure from 103 ± 7 to 184 ± 17 mmHg. For the Cat transgenic-overexpressing mice, the catalase transgene was constructed in

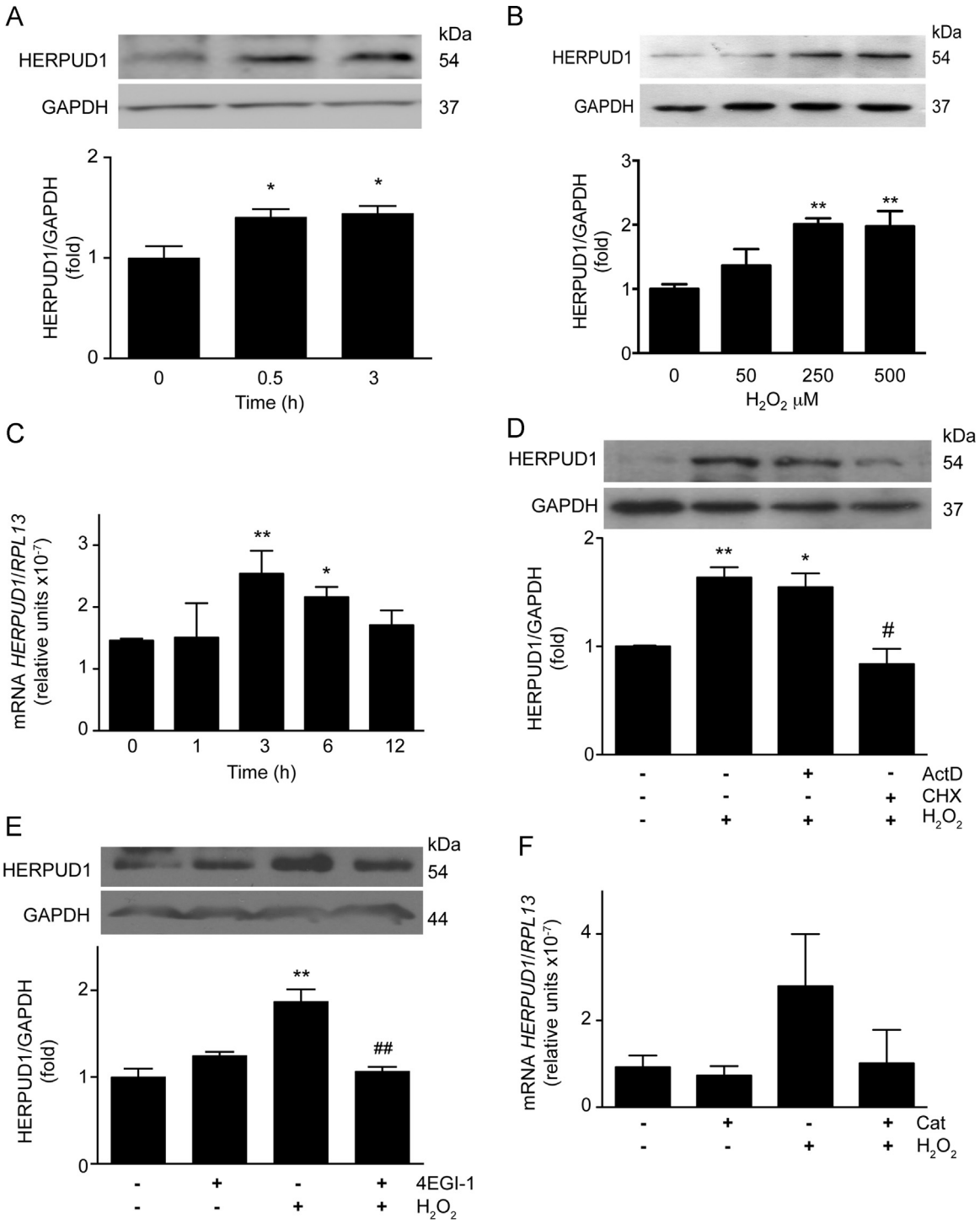

Fig. 1. Oxidative stress by H_2O_2 induces HERPUD1 by regulating transcription and translation. (A) HeLa cells were treated with H_2O_2 (500 μM) at indicated times. (B) HeLa cells were treated for 3 h with different concentrations of H_2O_2. HERPUD1 protein level was determined by Western blot and normalized using GAPDH. (C) HeLa cells were treated with H_2O_2 (500 μM) at indicated times, and *HERPUD1* mRNA levels were determined by RT qPCR. Results were normalized using the *RPL13* housekeeping gene. (D) HeLa cells were pretreated with cycloheximide (CHX, 20 μM, translation inhibitor) or actinomycin D (ActD, 20 μM, gene transcription inhibitor) for 30 min and then treated with H_2O_2 (500 μM) for 30 min. (E) HeLa cells were pretreated with 4EGI-1 (60 μM) for 30 min and then treated with H_2O_2 (500 μM) for 30 min. HERPUD1 protein level was determined by Western blot and normalized using GAPDH. (F) HeLa cells were pretreated with catalase (Cat, 2000 units) for 30 min and then treated with H_2O_2 (500 μM) for 30 min. *HERPUD1* mRNA levels were determined by RT qPCR and normalized using *RPL13* transcript. Values represent the mean ± SEM of 3 to 5 independent experiments; $^{*}p < 0.05$ and $^{**}p < 0.01$ vs. 0 h or control; $^{\#}p < 0.05$ and $^{\#\#}p < 0.01$ vs. H_2O_2-treated cells.

the pBSCX1-LEL plasmid vector. The final construct consisted of the strong universal promoter CX1, green fluorescent protein (GFP) cDNA with a stop codon flanked by loxP DNA cis-elements, and the human catalase cDNA. With this transgene, a line of transgenic mice (Tgflox-cat-SMC) mice was generated at the Emory University Transgenic Mouse Core Facility, as it has been previously described [31].

2.4. Extraction of RNA and gene expression analysis

Total RNA was obtained from HeLa cells using TRIzol reagent (Invitrogen, 15596-026). cDNA was prepared from 1 μg of RNA, using SuperScript II enzyme (Invitrogen, A13268), according to manufacturer protocol. Real-time PCR was performed using Stratagene Mx3000P (Stratagene) using the Brilliant III Ultra-Fast

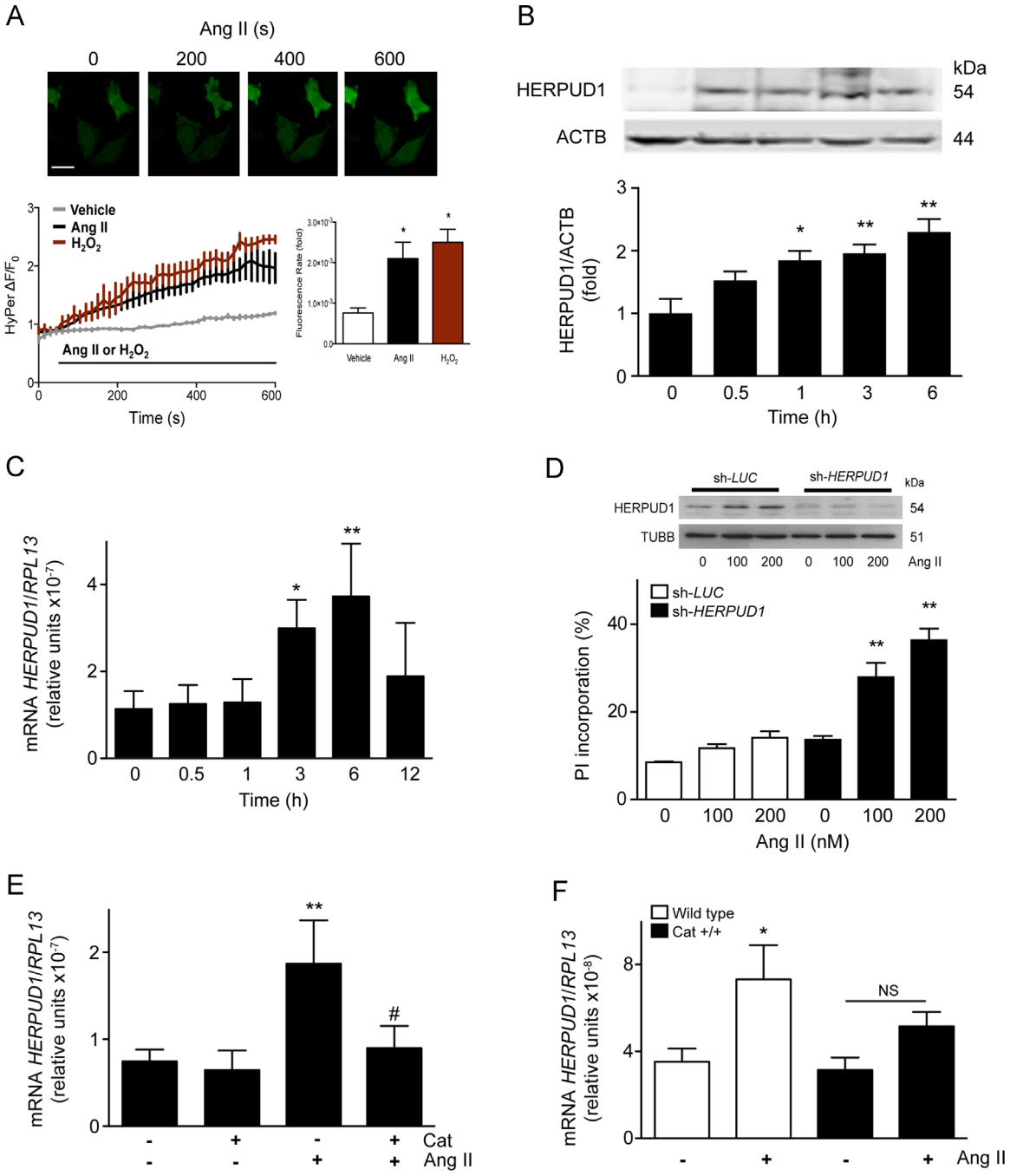

Fig. 2. Ang II induces HERPUD1 *in vitro* and *in vivo* by a ROS-dependent mechanism. (A) HeLa cells were transfected with a plasmid encoding HyPer. Transfected cells were left untreated, treated with Ang II (100 nM) or H_2O_2 (500 μM) and fluorescence was recorded using confocal microscopy (excitation/emission: 420/500 nm). Values were expressed as $(F-F_0)/F_0$. In the upper panel are displayed representative images of the Ang II treatment. (B) HeLa cells were treated with Ang II (100 nM) at the indicated times. HERPUD1 protein level was determined by Western blot and normalized using β-actin (ACTB). (C) HeLa cells were treated with Ang II (100 nM) at indicated times, and *HERPUD1* mRNA levels were determined by RT qPCR. Results were normalized using the *RPL13* housekeeping gene. (D) sh-*Luc* or sh-*HERPUD1* HeLa cells were treated with Ang II (0–200 nM). Cell death was assessed by propidium iodide (PI) incorporation using flow cytometry. In the upper panel are displayed a representative Western blot of the cells used in this assay. (E) HeLa cells were pretreated with catalase (Cat, 2000 units) for 30 min and then treated with Ang II (100 nM) for 3 h. *HERPUD1* mRNA levels were determined by RT qPCR and normalized using *RPL13* transcript. (F) Wild-type mice and catalase-overexpressing mice ($CAT^{+/+}$) were treated with saline or Ang II using an Alzet mini-osmotic pump at a dose of 0.75 mg/kg/day for 7 days. Animals were euthanized and aortas extracted. *HERPUD1* mRNA levels were analyzed in total mRNA from aorta tissue and normalized using *RPL13* transcript. Values represent the mean ± SEM of 3–5 independent experiment; $^{*}p < 0.05$ and $^{**}p < 0.01$ vs. 0 h or respective control; $^{\#}p < 0.05$ vs. Ang II-treated cells.

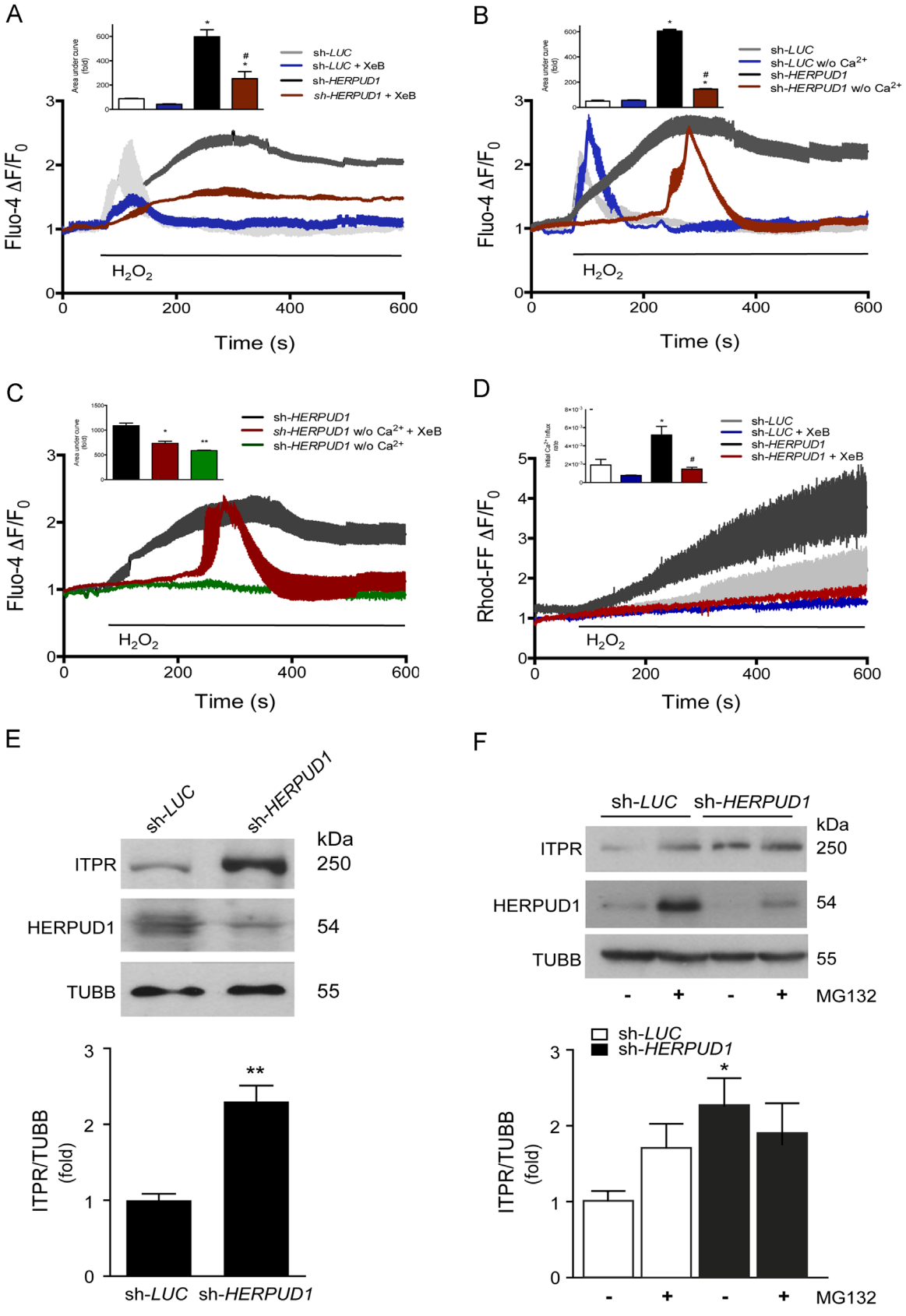
A
Area under curve (fold)
sh-LUC
sh-LUC + XeB
sh-HERPUD1
sh-HERPUD1 + XeB
Fluo-4 ΔF/F0
H2O2
Time (s)
B
sh-LUC
sh-LUC w/o Ca2+
sh-HERPUD1
sh-HERPUD1 w/o Ca2+
C
sh-HERPUD1
sh-HERPUD1 w/o Ca2+ + XeB
sh-HERPUD1 w/o Ca2+
D
Initial Ca2+ influx rate
Rhod-FF ΔF/F0
E
sh-LUC
sh-HERPUD1
kDa
ITPR
250
HERPUD1
54
TUBB
55
ITPR/TUBB (fold)
F
MG132

QPCR and QRT-PCR Master Mix amplification kit (Agilent Technologies, 4309155). The primers used were: human *HERPUD1* forward 5′-CGTTGTTATGTACCTGCATC-3′; human *HERPUD1* reverse 5′- TCAGGAGGAGGACCATCATTT-3′; human ribosomal protein 13a (*RPL13*) forward 5′-CCTGGAGGAGAAGAGGAAAGAGA-3′; human *RPL13* reverse 5′-TTGAGGACCTCTGTGTATTTGTCAA-3′; mouse *HERPUD1* forward 5′-CAGTTGGAGTGTGAGT-3′; mouse *HERPUD1* reverse 5′-CAACAGCAGCTTCCCAGAATA-3′; mouse *RPL13* forward 5′-ATGACAAGAAAAAGCGGATG-3′; mouse *RPL13* reverse 5′-CTTTTCTGCCTGTTTCCGTA-3′. All primers used showed optimal amplification efficiency (90% to 110%). PCR amplification of the housekeeping gene *RPL13* was performed as a control. CT value was determined by MxPro software when fluorescence was 25% higher than background. PCR products were verified by melting-curve analysis.

2.5. Western blot

Equal amounts of protein from complete cell extracts were separated by SDS-PAGE (10% polyacrylamide gels) and electro-transferred to nitrocellulose. Membranes were blocked with 5% milk TBS-T. Membranes were incubated with primary antibodies at 4 °C and blotted with horseradish peroxidase-linked secondary antibodies (1:5000 in 1% [w/v] milk in TBS-T). Signals were detected using EZ-ECL (Biological Industries, 20-500-1000A, 20-500-1000B) and quantified by scanning densitometry. Protein content was normalized with β-tubulin (TUBB), β-actin (ACTB) or GAPDH.

2.6. Cell viability and apoptosis assays by flow cytometry

The integrity of the sh-*Luc* and sh-*HERPUD1* HeLa cell plasma membranes was assessed by the ability of cells to exclude PI. Cells were collected by centrifugation, washed once with PBS, and re-suspended in PBS containing 0.1 mg/mL PI. The levels of PI incorporation were quantified on a FACScan flow cytometer. Cell size was evaluated by forward-angle light scattering (FSC). PI-negative cells of normal size were considered alive. Sub-G1 population was determined in HeLa cells. The cells were collected, pooled, permeabilized with methanol for 24 h, treated with RNase for 1 h and then 2 μL PI (25 μg/mL) was added prior to flow cytometry analysis. A total of five thousand cells per sample were analyzed [32,33].

2.7. LDH release

Lactate dehydrogenase (LDH) activity in the culture medium was assessed using a CytoTox 96w Non-Radioactive Cytotoxicity Assay (Promega, Madison, WI, USA), following the manufacturer's instructions.

2.8. Mitochondrial membrane potential and ROS determination by flow cytometry

Mitochondrial membrane potential (Ψ_{mt}) and ROS were measured with TMRM (200 nM, 30 min) or CM-H_2DCFDA (10 mM, 30 min), respectively. Mean population fluorescence was measured by flow cytometry using a FACScan system (Becton–Dickinson). CCCP or H_2O_2 were used as positive control for Ψ_{mt} loss or ROS, respectively. Data were analyzed using the Cell Quest (BD) software.

2.9. Cytoplasmic and mitochondrial Ca^{2+}

To determine cytoplasmic and mitochondrial Ca^{2+} kinetics, time-lapse images were obtained from HeLa cells preloaded with Fluo-4AM (Invitrogen, F-14201), Fura-2AM (Invitrogen, F-1221) or Rhod-FF (Invitrogen, R23983) using a Zeiss LSM 5 Pa/Axiovert 200 microscope, as previously described [34–36].

2.10. Intracellular ROS detection using confocal microscopy

HyPer-transfected cells were plated to glass-bottom dishes and analyzed by confocal microscopy as previously described [37]. The fluorescence (excitation/emission: 420/500 nm) was examined under confocal microscopy.

2.11. Immunofluorescence studies for cytochrome-c release

Cyt-C release was evaluated by immunofluorescence as described previously [38,39]. HeLa cells grown on coverslips were fixed with PBS containing 4% paraformaldehyde for 10 min, permeabilized with 0.3% Triton X-100 for 10 min, and blocked for 1 h with 5% BSA in PBS. Cells were then incubated with anti-Cyt-C antibody at 1:400 and revealed with anti-mouse IgG-Alexa 488. Coverslips were mounted in DakoCytomation fluorescence mounting medium (DakoCytomation, Carpinteria, CA) and visualized by confocal microscope (Carl Zeiss Axiovert 135, LSM Microsystems). Two blinded investigators quantified the number of cells exhibiting a punctuated or localized pattern as well as a diffuse one. Once we have both data sets (n: 4 independent experiments), they were averaged and graphed. Additionally, total fluorescence (area) was also quantified for all the conditions analyzed to evaluate the amount of Cyt-C expressed.

2.12. Click chemistry

RNA transcription and protein translation in cells treated with ActD and CHX, respectively, were measured using Click Chemistry following manufacturer's instructions. Briefly, RNA transcription was assayed using the Click-iT® RNA Alexa Fluor® 488 Imaging Kit (Life Technologies) that employs an alkyne-modified nucleoside EU (5-ethynyl uridine), which is supplied to cells and incorporated into nascent RNA [40]. For the analysis of protein translation we used the Click-iT® HPG Alexa Fluor® 488 Protein Synthesis Assay Kit, which uses L-homopropargylglycine (HPG), a methionine alkyne analog; and Alexa Fluor® 488 azide. The HPG is fed to cultured cells and incorporated into proteins during active protein synthesis. Addition of the Alexa Fluor® 488 azide leads to a

Fig. 3. HERPUD1 regulates intracellular and mitochondrial Ca^{2+} by controlling ITPR protein levels. (A) sh-*Luc* (control) or sh-*HERPUD1* HeLa cells were pretreated or not with xestospongin B (XeB, 100 μM, IP3R antagonist), preloaded with Fluo-4AM (5.4 μM, cytosolic Ca^{2+} probe) for 30 min, treated with H_2O_2 and then visualized under a confocal microscope. Inset: Quantitation of the area under the curve of the kinetics shown in the Figure. (B) sh-*Luc* (control) or sh-*HERPUD1* HeLa cells were preloaded with Fluo-4AM (5.4 μM) and incubated in Ca^{2+}-containing (w/Ca^{2+}) or Ca^{2+}-free (w/o Ca^{2+}) resting media. Inset: Quantitation of the area under the curve of the kinetics depicted in the Figure. (C) sh-*Luc* (control) or sh-*HERPUD1* HeLa cells were preloaded with Fluo-4AM (5.4 μM), pretreated or not with xestospongin B (XeB, 100 μM), and incubated in Ca^{2+}-containing (w/Ca^{2+}) or Ca^{2+}-free (w/o Ca^{2+}) resting media. Inset: Quantitation of the area under the curve of the kinetics depicted in the Figure. (D) sh-*Luc* (control) or sh-*HERPUD1* HeLa cells were pretreated or not with xestospongin B (XeB, 100 μM) and preloaded with Rhod-FF (5 μM, a mitochondrial Ca^{2+} probe) for 30 min. Using a fluorescence microscopy equipped with a CDD camera, serial Ca^{2+} kinetics in a single cell were recorded, and the relative total fluorescence [ratio of fluorescence difference, stimulated – baseline (F_i–F_o), to baseline value (F_o)] as a function of time was calculated for each image. After recording 80 s of baseline, cells were stimulated with H_2O_2 (500 μM). Inset: Quantitation of the slopes (Initial Ca^{2+} influx rate) of the kinetics depicted in the Figure. (E) Total protein extracts were prepared from sh-*Luc* (control) or sh-*HERPUD1* HeLa cells. ITPR and HERPUD1 levels were determined by Western blot. (F) sh-*Luc* (control) or sh-*HERPUD1* HeLa cells were preincubated with MG132 (100 μM, proteasome inhibitor) for 30 min. Total protein extracts were prepared, and ITPR and HERPUD1 levels were determined by Western blot. Values represent the mean ± SEM of 3 to 5 independent experiments; $^{*}p < 0.05$ and $^{**}p < 0.01$ vs. sh-*Luc*; $^{\#}p < 0.05$ vs. sh-*HERPUD1*.

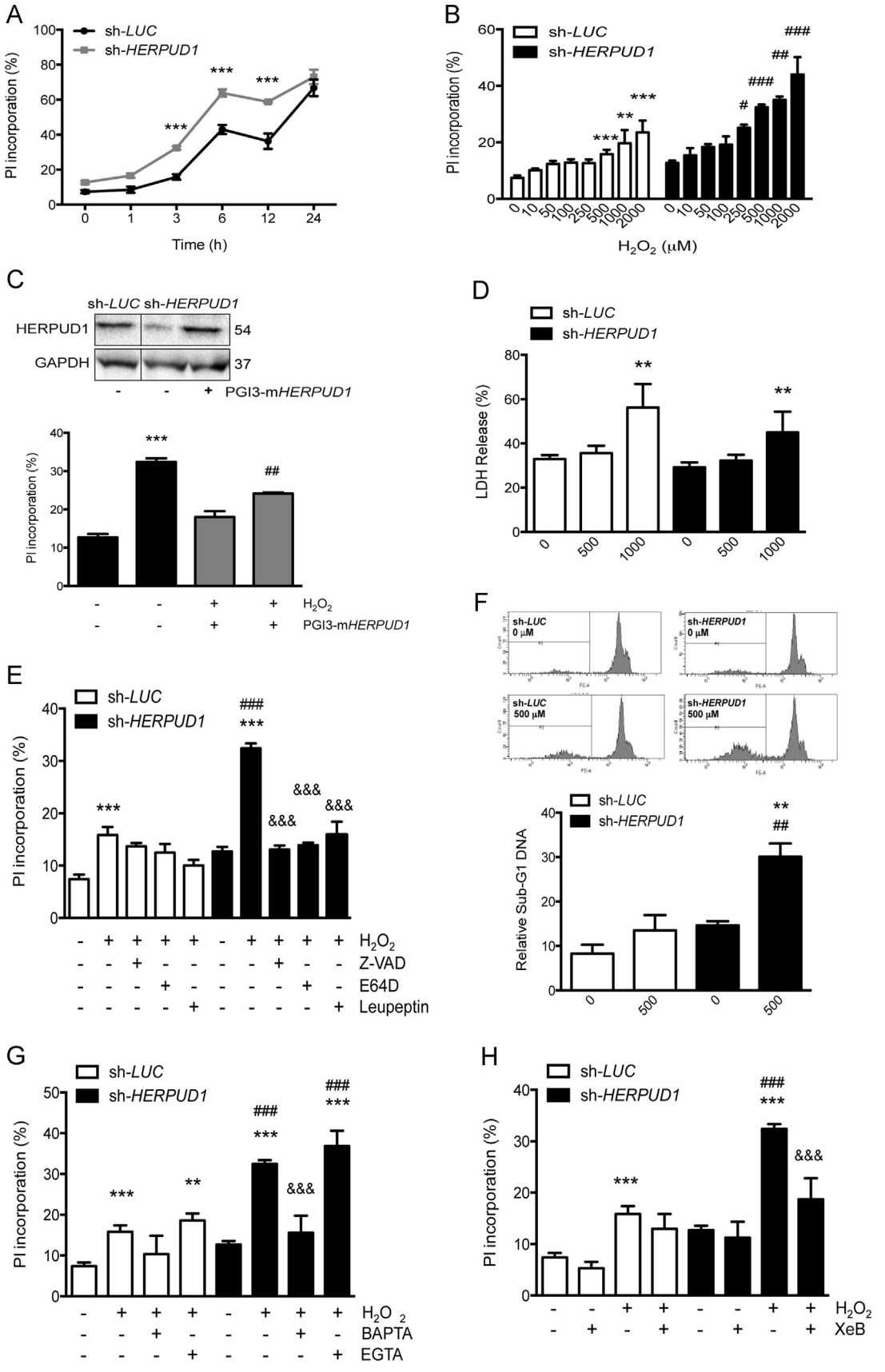
A
sh-LUC
sh-HERPUD1
PI incorporation (%)
Time (h)
B
sh-LUC
sh-HERPUD1
PI incorporation (%)
H2O2 (μM)
C
sh-LUC sh-HERPUD1
HERPUD1
GAPDH
54
37
PGI3-mHERPUD1
PI incorporation (%)
H2O2
PGI3-mHERPUD1
D
sh-LUC
sh-HERPUD1
LDH Release (%)
E
sh-LUC
sh-HERPUD1
PI incorporation (%)
H2O2
Z-VAD
E64D
Leupeptin
F
sh-LUC 0 μM
sh-HERPUD1 0 μM
sh-LUC 500 μM
sh-HERPUD1 500 μM
sh-LUC
sh-HERPUD1
Relative Sub-G1 DNA
G
sh-LUC
sh-HERPUD1
PI incorporation (%)
H2O2
BAPTA
EGTA
H
sh-LUC
sh-HERPUD1
PI incorporation (%)
H2O2
XeB

chemoselective ligation or "click" reaction between the green fluorescent azide and the alkyne, allowing the modified proteins to be detected by confocal or fluorescence microscopy.

2.13. Statistical analysis

Data are mean ± SEM of the indicated sample size (n). Multiple groups were analyzed using one-way ANOVA followed by a protected Bonferroni's test. Statistical significance was set as $p < 0.05$.

3. Results

3.1. HERPUD1 protein is upregulated in HeLa cells treated with H_2O_2 in a time-dependent manner

HERPUD1 protein levels were evaluated in HeLa cells treated with 500 μM of H_2O_2 at indicated times. This concentration did not compromise cell viability. Treating HeLa cells with 500 μM H_2O_2 increased HERPUD1 protein levels (Fig. 1A). This response was not cell-specific, as MEF cells behaved similarly (Fig. S2). In a dose-response curve evaluated after 30 min of treatment, HERPUD1 protein level increased with administration of 250–500 μM H_2O_2 (Fig. 1B).

Gene expression analysis using qPCR showed increased *HERPUD1* mRNA after 3 h treatment with H_2O_2 (Fig. 1C). These data suggest that the increased HERPUD1 protein levels at 3 h of H_2O_2 treatment could be attributable to an increase in *HERPUD1* mRNA levels. However, shorter H_2O_2 treatment times (30 min) did not affect *HERPUD1* transcripts levels. Using ActD (a well-known gene transcription inhibitor) and the translation inhibitor CHX, the effect of H_2O_2 on HERPUD1 protein expression was studied after short (30 min) and long (3 h) intervals. While CHX treatment completely inhibited the increase in HERPUD1 protein levels, ActD treatment only partially inhibited this increase (Fig. 1D). These data suggest that the rapid HERPUD1 protein increase observed at 30 min is probably due to enhanced translation of already-synthesized *HERPUD1* mRNA. To corroborate the proper interpretation of these results, we checked that ActD and CHX treatments were effective at inhibiting gene transcription and translation, respectively (Fig. S3A and B).

The translation initiator factor eIF4E is involved in rapid cell responses against oxidative stress [41]. Therefore, we reasoned that EIF4E regulation mediated the rapid increase in HERPUD1 after an oxidative insult such as H_2O_2. Indeed, we observed that the H_2O_2-induced increase in HERPUD1 level was completely abolished in cells pretreated with 4EGI-1, which inhibits the binding of eIF4E to its effector eIF4G (Fig. 1E). Moreover, preincubating HeLa cells with a soluble form of catalase (Cat) shows a not significant tendency to blunt the increase in *HERPUD1* mRNA expression induced by the H_2O_2 treatment (Fig. 1F), together with inhibiting the ROS intracellular production triggered by H_2O_2 itself, without changing the total protein levels of HERPUD1 (Fig. S3C-D). Taken together, these data show that HERPUD1 is upregulated in response to exogenous H_2O_2 and that this increase may involve both the translation of preexisting mRNA (fast response) and *de novo* synthesized mRNA (slow response).

3.2. HERPUD1 is upregulated in response to angiotensin II in vitro and in vivo

In order to explore the physiological relevance of this mechanism, HeLa cells were treated with angiotensin II (Ang II), a known physiological H_2O_2 inducer in a variety of cell types including HeLa cells [42]. In fact, treatment with Ang II (100 nM) increased intracellular H_2O_2 production as measured by increased HyPer-mediated fluorescence, a response that is similar to the one observed with the H_2O_2 treatment (Fig. 2A). Importantly, Ang II was also sufficient to increase HERPUD1 at the protein (Fig. 2B) and mRNA (Fig. 2C) levels. HERPUD1 protein levels increased after 1 h of Ang II treatment and remained elevated until 6 h, whereas *HERPUD1* mRNA increased after 3 h post-stimulation. Treatment of HeLa cells with 100 or 200 nM Ang II for 24 h did not affect cell viability. However, in *HERPUD1* knockdown HeLa cells, but not in control cells, Ang II induced cell death in a dose dependent manner (Fig. 2D). To confirm the role of H_2O_2 in Ang II-mediated HERPUD1 upregulation, cells were again preincubated with the soluble form of Cat. As expected, Cat blunted the increase in *HERPUD1* mRNA expression (Fig. 2E).

HERPUD1 upregulation triggered by Ang II was also studied in vivo. *HERPUD1* mRNA levels were increased in the aorta tissue of wild-type mice treated with Ang II for 2 weeks (0.75 mg/kg/day using Alzet minipumps). This increase was significantly blunted in Cat-overexpressing mice (Fig. 2F). Taken together, these data show that HERPUD1 is upregulated in response to Ang II by a mechanism involving intracellular production of H_2O_2 both *in vitro* and *in vivo*.

3.3. HERPUD1 regulates ITPR-dependent Ca^{2+} release from the ER

Because H_2O_2 increases intracellular and mitochondrial Ca^{2+} levels [43] and the HERPUD1 protein plays a role in Ca^{2+} homeostasis regulation [24,28,29] we investigated the role of HERDUP1 in H_2O_2-induced Ca^{2+} release from the ER. To this end, we recorded Ca^{2+} kinetics after a pulse of 500 μM H_2O_2 in control cells and *HERPUD1* knockdown HeLa cells. Using Fluo-4 as a cytosolic Ca^{2+} probe, we found that H_2O_2 increases cytoplasmic Ca^{2+} levels, with a kinetic plot characterized by a fast response with a single peak and a quick return to baseline. However, the kinetic plot was different in sh-*HERPUD1* cells, showing a slower Ca^{2+} transient that extended over time, suggesting a more prolonged Ca^{2+} release from the ER. All these data were further corroborated by the quantification and statistical comparison of the area under the curve and the slope (initial Ca^{2+} influx rate) of these kinetic experiments (Figs. 3A and S4A). Additionally, a very similar result was obtained using Fura2, a quantitative Ca^{2+} probe as shown in Fig. S4C.

Fig. 4. HERPUD1 decreases H_2O_2-induced cell death by a Ca^{2+}-dependent mechanism. (A) sh-*Luc* or sh-*HERPUD1* HeLa cells were treated with H_2O_2 (500 μM). At indicated times, cell death was assessed by propidium iodide (PI) incorporation using flow cytometry. (B) sh-*Luc* or sh-*HERPUD1* HeLa cells were treated with different H_2O_2 concentrations ranging from 0 to 2,000 μM and incubated for 3 h. (C) sh-*HERPUD1* HeLa cells were transiently transfected with a plasmid overexpressing mouse *HERPUD1* (PGI3-m*HERPUD1*; OriGene Technologies, Rockville, SC114911). Cells were treated with H_2O_2 (500 μM) for 3 h. Cell death was determined as indicated above. (D) sh-*Luc* or sh-*HERPUD1* HeLa cells were treated with different H_2O_2 concentrations ranging from 0 to 1000 μM, incubated for 3 h and then LDH release was measured in the media. (E) sh-*Luc* or sh-*HERPUD1* HeLa cells were preincubated with ZVAD (20 μM, caspase inhibitor), E64D (10 μM, calpain inhibitor) or leupeptin (100 μM, general protease inhibitor) for 30 min and then treated with H_2O_2 (500 μM) for 3 h. (F) sh-*Luc* or sh-*HERPUD1* HeLa cells were treated with H_2O_2 500 μM for 3 h, trypsinized, fixed, treated with PI and then assessed by flow cytometry in order to evaluate Sub-G1 DNA. (G) sh-*Luc* or sh-*HERPUD1* HeLa cells were pretreated with BAPTA-AM (20 μM, intracellular Ca^{2+} chelating agent) or EGTA (5 mM, Ca^{2+} chelator) for 30 min and then treated with H_2O_2 (500 μM) for 3 h. (H) sh-*Luc* or sh-*HERPUD1* HeLa cells were pretreated or not with xestospongin B (XeB, 100 μM, IP_3R antagonist). Values represent the mean ± SEM of 3 to 10 independent experiments; $^{*}p < 0.05$, $^{**}p < 0.01$ and $^{***}p < 0.001$ vs. sh-*Luc*; $^{\#}p < 0.05$, $^{\#\#}p < 0.01$ and $^{\#\#\#}p < 0.001$ vs. respective control and $^{\&\&\&}p < 0.001$ vs. sh-*HERPUD1* H_2O_2.

We used XeB, a specific ITPR antagonist, to establish the role of the ITPR in Ca^{2+} signaling induced by H_2O_2 and its relationship with HERPUD1. While XeB completely abolished the intracellular Ca^{2+} transient in sh-*Luc* cells, the amplitude of the Ca^{2+} signal decreased in sh-*HERPUD1* cells. This signal did not completely disappear, probably due to the involvement of other Ca^{2+} channels (Fig. 3A and S4A). These results support a role for ITPR in the Ca^{2+} kinetics produced by H_2O_2 and suggest that HERPUD1 may be involved in this regulation. To better define the Ca^{2+} kinetics previously observed, we compared the cytosolic Ca^{2+} kinetics in Ca^{2+}-containing and Ca^{2+}-free media to study the influence of external Ca^{2+} on these signals. Figs. 3B and S4 B shows that the use of a Ca^{2+}-free medium did not affect Ca^{2+} kinetics in sh-*Luc* control cells, suggesting that the kinetics in these cells are mainly dependent on internal Ca^{2+} stores. However, the Ca^{2+} kinetics produced in the sh-*HERPUD1* cells showed two components, the first dependent on ITPR-related internal stores and the second dependent on extracellular Ca^{2+} influx. To test this finding, Ca^{2+} kinetics were studied in response to H_2O_2 using Ca^{2+}-free medium in sh-*HERPUD1* cells preincubated with XeB (Fig. 3C). Under this condition, the Ca^{2+} signal completely disappeared, confirming that HERPUD1 is involved in the regulation of both ITPR and external Ca^{2+} influx in the cells lacking HERPUD1.

3.4. HERPUD1 controls Ca^{2+} transfer from the ER to mitochondria by regulating ITPR

Because the ITPR participates in the transfer of Ca^{2+} between the ER and mitochondria, we studied the role of HERPUD1 in the mitochondrial Ca^{2+} influx in response to H_2O_2. Sh-*HERPUD1* and sh-*Luc* HeLa cells were preincubated with Rhod-FF, a Ca^{2+} probe with a preferential mitochondrial localization. In both sh-*Luc* and sh-*HERPUD1* cells, we observed a constant Ca^{2+} influx into the mitochondria in response to H_2O_2 stimulation. However, this influx was faster in *HERPUD1* knockdown HeLa cells than in controls, as we deduce from the curves observation and the quantitation of their slopes (initial Ca^{2+} influx rates). Furthermore, the mitochondrial Ca^{2+} signal decreased completely both in control sh-*Luc* and sh-*HERPUD1* cells treated with XeB (Fig. 3D), thus confirming that ITPR is important to the Ca^{2+} influx from the ER to mitochondria and that the differences in mitochondrial Ca^{2+} signals observed in the sh-*HERPUD1* cells are due to a functional deregulation of the ITPR. To further corroborate the ITPR's engagement in mitochondrial Ca^{2+} kinetics, histamine was used to increase ITPR levels and Ca^{2+} movement from the ER to the mitochondria via ITPR.[16] Sh-*HERPUD1* cells treated with a pulse of histamine exhibited a longer kinetic with higher amplitude than control cells. Both in sh-*HERPUD1* and sh-*Luc* cells, mitochondrial Ca^{2+} signals were abolished with XeB (Fig. S4D), confirming that HERPUD1 regulates ITPR function and Ca^{2+} influx from ER to mitochondria.

In a previous study, Belal et al. showed that HERPUD1 modulates intracellular Ca^{2+} levels through the regulation of ITPR degradation; therefore we then studied whether cells with lower levels of HERPUD1 showed altered ITPR levels [28]. As shown in Fig. 3E sh-*HERPUD1* cells showed a significant increase in ITPR levels compared to sh-*Luc* cells. This result may explain the differences observed in the Ca^{2+} kinetics triggered by H_2O_2 in the sh-*HERPUD1* cells and the results obtained when the ER Ca^{2+} levels were depleted with thapsigargin in cells incubated in Ca^{2+} free media. Under these conditions (Fig. S4E), the H_2O_2-triggered Ca^{2+} signal was almost abolished in the sh-*Luc* and sh-*HERPUD1* cells despite that the levels of cytosolic Ca^{2+} post the thapsigargin challenge were considerably higher in the sh-*HERPUD1* cell line.

Finally, HERPUD1 protein levels increased in sh-*Luc* and sh-*HERPUD1* HeLa cells treated with MG132 (100 μM, 4 h), an inhibitor of proteasomal activity and an ER stress inducer (Fig. 3F). MG132 also increased the ITPR levels both in sh-*Luc* cells as sh-*HERPUD1* cells. This evidence suggests that HERPUD1 is involved in ITPR degradation via the proteasome.

3.5. HERPUD1 exerts a Ca^{2+}-dependent cytoprotective effect against H_2O_2

Deregulation of ROS and intracellular Ca^{2+} levels affects cell survival against a variety of insults. We investigated whether HERPUD1 also exerts a cytoprotective effect against H_2O_2. Sh-*HERPUD1* cells treated with 500 μM H_2O_2 for 3 h showed significantly more cell death than control cells (Fig. 4A). This difference persisted until 12 h post-treatment. We next established the relationship between cell death and H_2O_2 concentration at 3 h. Differences in cell death in *sh-HERPUD1* vs. sh-*Luc* were observed in concentrations ranging from 250 μM to 2 mM H_2O_2 (Fig. 4B). A similar result was observed when viability was assessed using the Trypan blue assay (Fig. S5). These data suggest that HERPUD1 exerts a cytoprotective effect against the oxidative stress induced by H_2O_2. To corroborate this data, sh-*HERPUD1* cells were transiently transfected with a plasmid-expressing mouse *HERPUD1* (PGI3-m*HERPUD1*). The sh-m*HERPUD1*-transfected cells recovered the HERPUD1 protein levels and exhibited less cell death after treatment with H_2O_2 (Fig. 4C). In order to elucidate the mechanism by which HERPUD1 participates in cell protection, different techniques were used to elucidate the cell death pathways stimulated by H_2O_2 in our system. We first tested the participation of necrosis by measuring LDH release after the H_2O_2 treatment, but we did not observe any changes under our conditions (H_2O_2 500 μM) or between the sh-*Luc* and sh-*HERPUD1* cells (Fig. 4D). Only after the treatment of both cell lines with 1000 μM of H_2O_2, they showed an increase of LDH. However, this result did not explain the differences observed between the cell lines in Fig. 4A and B. Next we tested three different chemical inhibitors of cell death. ZVAD (a caspase inhibitor), E64D (a calpain inhibitor), and leupeptin (a general protease inhibitor) were able to reverse the cell death caused by H_2O_2 in the sh-*HERPUD1* cells (Fig. 4E), suggesting that apoptosis can be the main type of cell death triggered by H_2O_2 in our experimental model. Additionally, the measurement of Sub-G1 DNA population corroborated the importance of apoptosis in our experimental setting (Fig., 4F), thus confirming our previous results. Interestingly, pre-incubation with BAPTA-AM, an intracellular Ca^{2+} chelating agent, resulted in a significant inhibition of cell death in the sh-*HERPUD1* cells (Fig. 4D). This result suggests that the increased sensitivity to cell death observed in the sh-*HERPUD1* cells could be explained by intracellular Ca^{2+} deregulation, which would in turn cause greater cell sensitivity to oxidative stress. Additionally, the use of EGTA, an extracellular Ca^{2+} chelating agent, did not blunt the H_2O_2-induced sh-*HERPUD1* cell death (Fig. 4E). This last result suggests that increased death in the sh-*HERPUD1* cells may involve the release of Ca^{2+} from intracellular stores and not Ca^{2+} influx from the extracellular media, connecting these results with those obtained through Ca^{2+} measurements.

One of the best-known pathways that triggers cell death in response to oxidative stress involves increased mitochondria Ca^{2+} influx, which causes mitochondrial Ca^{2+} overload and MPTP opening and consequent cell death [44,45]. As we had already established that the ITPR was responsible for the cytosolic and mitochondrial Ca^{2+} increases induced by H_2O_2 and that these signals were deregulated in sh-*HERPUD1* cells, we studied the involvement of ITPR in increased sensitivity to H_2O_2. Sh-*HERPUD1* and sh-*Luc* cells were treated with XeB and then with H_2O_2 for 3 h. As previously shown, sh-*HERPUD1* cells were more sensitive to H_2O_2 than control cells. However, sh-*HERPUD1* cells pre-incubated

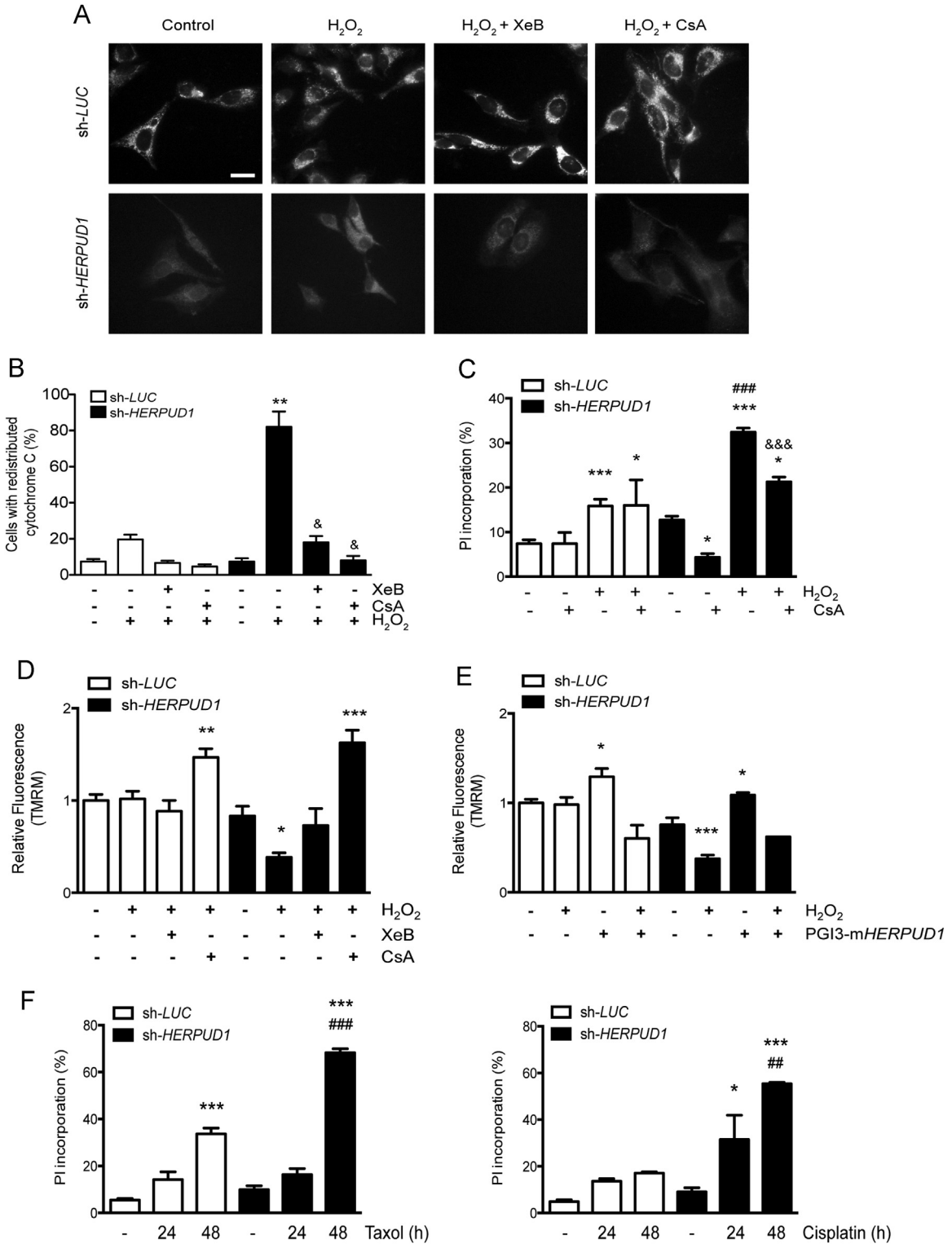

Fig. 5. HERPUD1 reduces H_2O_2-induced cell death by decreasing Ca^{2+}-dependent MPTP opening. (A) Representative confocal microscopy images of immunofluorescence against cytochrome C in sh-*Luc* or sh-*HERPUD1* HeLa cells treated with H_2O_2 (500 μM for 3 h), H_2O_2 + xestospongin B (XeB, 100 μM) or H_2O_2 + cyclosporine A (CsA, 100 μM). (B) Quantification of cytochrome c relocalization. (C) sh-*Luc* or sh-*HERPUD1* HeLa cells were preincubated with CsA (100 μM) for 30 min and then treated with H_2O_2 (500 μM for 3 h). Cell death was measured by PI incorporation using flow cytometry. (D) sh-*Luc* or sh-*HERPUD1* HeLa cells were preincubated with XeB (100 μM) or CsA (100 μM) for 30 min and then treated with H_2O_2 (500 μM for 3 h). Mitochondrial membrane potential (Ψ_{mt}) was measured in cells incubated with TMRM (400 nM) and then analyzed by flow cytometry. (E) sh-*HERPUD1* HeLa cells were transiently transfected with a plasmid overexpressing mouse *HERPUD1* (PGI3 m*HERPUD1*). Cells were treated with H_2O_2 (500 μM) for 3 h. Ψ_{mt} was determined as indicated above. (F) sh-*Luc* or sh-*HERPUD1* HeLa cells were treated with Taxol (50 nM) or Cisplatin (5 μg/μL) for 24–48 h, then cell death was measured by PI incorporation using flow cytometry. Values represent the mean ± SEM of 3 to 5 independent experiments; $^{*}p < 0.05$, $^{**}p < 0.01$ and $^{***}p < 0.001$ vs. sh-*Luc*; $^{\#\#}p < 0.01$ and $^{\#\#\#}p < 0.001$ vs. respective control and $^{\&}p < 0.05$ and $^{\&\&\&}p < 0.001$ vs. sh-*HERPUD1* H_2O_2.

with XeB showed significantly lower death rates than sh-*HERPUD1* cells without XeB after treatment with H_2O_2 (Fig. 4F). These data suggest that the increased sensitivity of the sh-*HERPUD1* cells is due to deregulation of intracellular Ca^{2+} levels, specifically by overregulation of the ITPR.

3.6. Increased apoptosis in sh-HERPUD1 HeLa cells after H_2O_2 is dependent on mitochondrial depolarization and MPTP opening

To understand the role of Ca^{2+} overload and HERDUP1 in H_2O_2-induced cell death, cytochrome C (Cyt-C) subcellular redistribution from the mitochondria to cytoplasm was used as readout of mitochondrial membrane potential loss due to MPTP opening [44,45]. As shown in Fig. 5A, sh-*Luc* cells under control conditions had a normal punctuated Cyt-C pattern that turned diffuse after treatment with H_2O_2 (Fig. 5A and B). In contrast, sh-*HERPUD1* cells showed a baseline redistribution of Cyt-C to the cytoplasm, indicating that these non-treated cells already exhibited increased mitochondrial permeability. Furthermore, the mitochondrial pattern of Cyt-C was completely lost in the cells treated with H_2O_2 (Fig. 5A and B). The total fluorescence levels associated to the Cyt-C protein showed a not significant decrease in the shHERPUD1 cells, from 1.00 ± 0.10 a.u. (arbitrary units) in the sh-Luc to 0.65 ± 0.07 a.u. in the sh-HERPUD1 condition, however, this decrease did not affect the loss of the punctuated pattern that the Cyt-C exhibited post H_2O_2 treatment, as it has been widely described by we and others [38,39]. Subsequently, to corroborate that Cyt-C redistribution occurred in response to an ITPR-dependent mitochondrial Ca^{2+} overload and MPTP opening, cells were preincubated with XeB or CsA, respectively. CsA is an inhibitor of MPTP opening [44,45]. Both inhibitors recovered the punctuated pattern observed in sh-*Luc* cells. Moreover, sh-*HERPUD1* cells recovered the baseline punctuated Cyt-C pattern, and both compounds prevented the redistribution induced by H_2O_2 (Fig. 5A and B). The increased cell death after H_2O_2 treatment was consistently blunted in sh-*HERPUD1* cells treated with CsA (Fig. 5C). Moreover, sh-HERPUD1 cells exhibited a decreased mitochondrial membrane potential, which was recovered after cells pre-incubation with XeB or CsA (Fig. 5D) and by the overexpression of HERPUD1 using the mouse protein (PGI3-m*HERPUD1*) (Fig. 5E). All of these data suggest that the increased cell death observed in sh-*HERPUD1*-treated cells is dependent on mitochondrial Ca^{2+} overload and the subsequent MPTP opening.

Finally, to test whether these effects were specific to H_2O_2 or due to a general increased sensibility to cell death of the sh-*HERPUD1* cells, HeLa cells were exposed to two chemotoxic agents (Taxol and Cisplatin). Both agents replicated the response to H_2O_2 (Fig. 5F), suggesting that the increased susceptibility observed in the sh-*HERPUD1* cells is part of a broad mechanism and not a specific effect to H_2O_2.

4. Discussion

HERPUD1 is an ER protein involved in the regulation of cellular homeostasis and in the degradation of proteins through the formation of ERAD complex in the proteasomal pathway [21–23,46,47]. HERPUD1 is also an early ER stress-induced protein, participating in the unfolded protein response (UPR) and Ca^{2+} homeostasis [21–24,28]. The present study provides the first demonstration of the role of HERPUD1 in the response against oxidative stress, which operates through maintenance of intracellular Ca^{2+} homeostasis and prevention of the cell death caused by increased production of intracellular ROS (Fig. 6).

In the literature, the relationship between HERPUD1 and oxidative stress is controversial, with only two works that have attempted to elucidate this issue. van Laar et al. described a slight increase in *HERPUD1* mRNA levels in response to H_2O_2 [48]. However, they discarded HERPUD1 as cytoprotective agent against oxidative stress because they could not replicate this observation in human fibroblasts. In contrast, we detected a consistent and significant increase in HERPUD1 protein and mRNA levels using the same concentration of H_2O_2. Moreover, we observed that the protein level increases showed a biphasic component and that the mRNA level changes were only significant after 3 h of treatment, times that were not evaluated by Van Laar et al. [48]. Interestingly, they also observed that osmotic stress, a known ROS endogenous inductor [49], was also able to induce HERPUD1. In the second work, Yan et al. observed that HERPUD1 was induced by reductive agents but not by H_2O_2 or paraquat [26]. In this case, we attribute the divergent results to the different experimental models and H_2O_2 concentrations and times studied. We also showed that the first rapid increase of HERPUD1 protein levels after 1 h of H_2O_2 treatment seems to depend on protein translation, specifically by a mechanism involving eIF4E factor (Fig. 1E). In contrast, the second increase of HERDUD1 protein levels (3 h) could be related to an

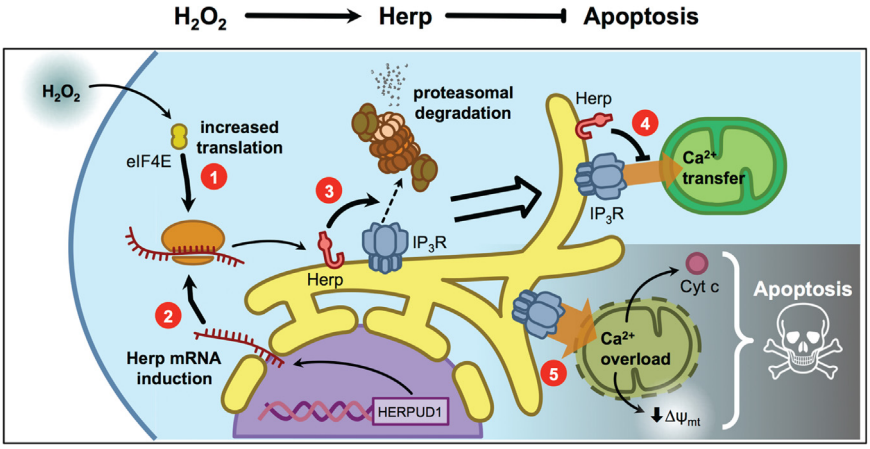

Fig. 6. Model of cell protection mediated by HERPUD1 against H_2O_2-induced apoptosis. (1) H_2O_2 induces a fast HERPUD1 (Herp) protein-level increase by transduction of preformed mRNA through an eIF4E-dependent mechanism and (2) a slow increase mediated by a transcriptional mechanism. (3) HERPUD1 induces inositol 1,4,5-trisphosphate receptor (IP3R) degradation by proteasome. (4) HERPUD1 reduces Ca^{2+} release from the endoplasmic reticulum, (5) reducing Ca^{2+} overload in the mitochondria, impeding mitochondrial transition pore opening and decreasing apoptosis.

increase in *HERPUD1* mRNA levels (Fig. 1C). Future work should clarify these points that under the current limitations of our study are beyond our scope.

More interesting was the finding using Ang II as an endogenous and physiological inductor of ROS. Ang II increased both HERPUD1 protein and mRNA levels *in vitro* and *in vivo*, effects inhibited by Cat overexpression (Fig. 2). Although there are previous reports connecting Ang II with the onset of ER stress [50], to our knowledge this is the first work showing a relationship between Ang II and HERPUD1. This result opens a new field of study where Ang II has an important pathophysiological role in the redox-induced signaling associated with the development of several cardiovascular diseases. It remains unknown whether HERPUD plays a role in ROS-dependent vascular diseases such as atherosclerosis and therefore whether HERPUD1 might be a novel pharmacological target.

Our results agree with several others works describing the role of HERPUD on Ca^{2+} signaling [24,28,29]. Importantly, our work corroborates the findings of Belal et al. that described the interaction between HERPUD1 and the ITPR [28]. Moreover, we show here that HERPUD1 protein levels are important in regulating cytosolic and mitochondrial Ca^{2+} signals induced by H_2O_2 and histamine, thus directly affecting the functional communication between the mitochondria and ER. In this context, we also established that HERPUD1 is an important regulator of mitochondrial Ca^{2+} overload, regulating mitochondrial permeability and cell death. Consistent with our data, Chigurupati et al. have shown that *HERPUD1* knockdown renders PC12 and MN9D cells more vulnerable to MPP^+-induced cytotoxic cell death by a mechanism involving upregulation of CHOP expression and ER Ca^{2+} depletion in the context of Parkinson disease [29]. Conversely, HERPUD1 overexpression confers protection by blocking MPP^+-induced CHOP up-regulation, ER Ca^{2+} store depletion, and mitochondrial Ca^{2+} accumulation [29]. Interestingly, we were able to reduce apoptosis in the sh-*HERPUD1* HeLa cells after H_2O_2 stimuli with ITPR and MPTP inhibitors (Fig. 5), which strongly suggesting that HERPUD1 control of cell death involves ER-dependent mitochondrial Ca^{2+} overload and the subsequent MPTP opening.

Finally, the recent work of Yan et al. described that HERPUD1 overexpression protects cells from ER stress but not oxidative stress [26]. Taken together with our results, these findings indicate that the mechanisms, by which HERPUD1 protects cells from ER and oxidative stress, although similar, are not the same. HERPUD1 seems to be a protein with a crucial role in maintaining cellular homeostasis. Any alteration of its levels (increase or decrease) triggers cellular imbalance, providing an elegant molecular mechanism that modulates different adaptive programs. Thus, in the case of ER stress, HERPUD1 is essential for avoiding the formation of toxic protein aggregates inside the cell [28]. During nutritional stress, HERPUD1 indirectly regulates protein autophagic degradation [27]. These data suggest that the role of HERPUD1 as a cytoprotective gene depends on the model and stimuli used.

Acknowledgments

This research was supported by CONICYT: FONDECYT Grants (1120212 to S.L., 11140470 to C.Q., 11130285 to R.T. and 3130749 to C.P.); FONDAP Grant (15130011 to S.L., M.C., R.T., A.S.M.) and the National Institutes of Health (HL113167 to A.S.M.). We are thankful for the Ph.D. or M.Sc. fellowships from CONICYT Chile to F.P., R.B., We also thank Fidel Albornoz and Gindra Latorre for their excellent technical assistance. None of the authors has a conflict of interest to declare.

Appendix A. Supplementary information

Supplementary data associated with this article can be found in the online version at http://dx.doi.org/10.1016/j.freeradbiomed.2015.11.024.

References

[1] B. Chetsawang, P. Kooncumchoo, P. Govitrapong, M. Ebadi, 1-Methyl-4-phenylpyridinium ion-induced oxidative stress, c-Jun phosphorylation and DNA fragmentation factor-45 cleavage in SK-N-SH cells are averted by selegiline, Neurochem. Int. 53 (2008) 283–288, http://dx.doi.org/10.1016/j.neuint.2008.08.007.

[2] J.L. Martindale, N.J. Holbrook, Cellular response to oxidative stress: signaling for suicide and survival, J. Cell. Physiol. 192 (2002) 1–15, http://dx.doi.org/10.1002/jcp.10119.

[3] Y. Saito, K. Nishio, Y. Ogawa, J. Kimata, T. Kinumi, Y. Yoshida, N. Noguchi, E. Niki, Turning point in apoptosis/necrosis induced by hydrogen peroxide, Free Radic. Res. 40 (2006) 619–630, http://dx.doi.org/10.1080/10715760600632552.

[4] G.C. Amberg, S. Earley, S.A. Glapa, Local regulation of arterial L-type calcium channels by reactive oxygen species, Circ. Res. 107 (2010) 1002–1010, http://dx.doi.org/10.1161/CIRCRESAHA.110.217018.

[5] T. Bruder-Nascimento, P. Chinnasamy, D.F. Riascos-Bernal, S.B. Cau, G.E. Callera, R.M. Touyz, R.C. Tostes, N.E. Sibinga, Angiotensin II induces Fat1 expression/activation and vascular smooth muscle cell migration via Nox1-dependent reactive oxygen species generation, J. Mol. Cell. Cardiol. 66 (2014) 18–26, http://dx.doi.org/10.1016/j.yjmcc.2013.10.013.

[6] Nguyen Dinh Cat, A. Montezano, A.C. Burger, D. Touyz, R.M. Angiotensin II, NADPH oxidase, and redox signaling in the vasculature, Antioxid. Redox Signal. 19 (2013) 1110–1120, http://dx.doi.org/10.1089/ars.2012.4641.

[7] K. Nakamura, K. Fushimi, H. Kouchi, K. Mihara, M. Miyazaki, T. Ohe, M. Namba, Inhibitory effects of antioxidants on neonatal rat cardiac myocyte hypertrophy induced by tumor necrosis factor-alpha and angiotensin II, Circulation 98 (1998) 794–799.

[8] I. Papparella, G. Ceolotto, D. Montemurro, M. Antonello, S. Garbisa, G. Rossi, A. Semplicini, Green tea attenuates angiotensin II-induced cardiac hypertrophy in rats by modulating reactive oxygen species production and the Src/epidermal growth factor receptor/Akt signaling pathway, J. Nutr. 138 (2008) 1596–1601.

[9] M. Takemoto, K. Node, H. Nakagami, Y. Liao, M. Grimm, Y. Takemoto, M. Kitakaze, J.K. Liao, Statins as antioxidant therapy for preventing cardiac myocyte hypertrophy, J. Clin. Investig. 108 (2001) 1429–1437, http://dx.doi.org/10.1172/JCI13350.

[10] A. Dikalova, R. Clempus, B. Lassegue, G. Cheng, J. McCoy, S. Dikalov, A. San Martin, A. Lyle, D.S. Weber, D. Weiss, W.R. Taylor, H.H. Schmidt, G.K. Owens, J. D. Lambeth, K.K. Griendling, Nox1 overexpression potentiates angiotensin II-induced hypertension and vascular smooth muscle hypertrophy in transgenic mice, Circulation 112 (2005) 2668–2676, http://dx.doi.org/10.1161/CIRCULATIONAHA.105.538934.

[11] K.K. Griendling, C.A. Minieri, J.D. Ollerenshaw, R.W. Alexander, Angiotensin II stimulates NADH and NADPH oxidase activity in cultured vascular smooth muscle cells, Circ. Res. 74 (1994) 1141–1148.

[12] P.N. Seshiah, D.S. Weber, P. Rocic, L. Valppu, Y. Taniyama, K.K. Griendling, Angiotensin II stimulation of NAD(P)H oxidase activity: upstream mediators, Circ. Res. 91 (2002) 406–413.

[13] E. Veal, A. Day, Hydrogen peroxide as a signaling molecule, Antioxid. Redox Signal. 15 (2011) 147–151, http://dx.doi.org/10.1089/ars.2011.3968.

[14] K. Horimoto, Y. Nishimura, T.M. Oyama, K. Onoda, H. Matsui, T.B. Oyama, K. Kanemaru, T. Masuda, Y. Oyama, Reciprocal effects of glucose on the process of cell death induced by calcium ionophore or H_2O_2 in rat lymphocytes, Toxicology 225 (2006) 97–108, http://dx.doi.org/10.1016/j.tox.2006.05.004.

[15] B. Bhandary, A. Marahatta, H.R. Kim, H.J. Chae, An involvement of oxidative stress in endoplasmic reticulum stress and its associated diseases, Int. J. Mol. Sci. 14 (2012) 434–456, http://dx.doi.org/10.3390/ijms14010434.

[16] I. Bejarano, J. Espino, D. Gonzalez-Flores, J.G. Casado, P.C. Redondo, J.A. Rosado, C. Barriga, J.A. Pariente, A.B. Rodriguez, Role of calcium signals on hydrogen peroxide-induced apoptosis in human myeloid HL-60 cells, Int. J. Biomed. Sci. 5 (2009) 246–256.

[17] L. Li, H. Tan, Z. Gu, Z. Liu, Y. Geng, Y. Liu, H. Tong, Y. Tang, J. Qiu, L. Su, Heat stress induces apoptosis through a Ca(2)(+)-mediated mitochondrial apoptotic pathway in human umbilical vein endothelial cells, Plos One 9 (2014) e111083, http://dx.doi.org/10.1371/journal.pone.0111083.

[18] M. Crompton, E. Barksby, N. Johnson, M. Capano, Mitochondrial intermembrane junctional complexes and their involvement in cell death, Biochimie 84 (2002) 143–152.

[19] J.P. Decuypere, G. Monaco, G. Bultynck, L. Missiaen, H. De Smedt, J.B. Parys, The IP(3) receptor-mitochondria connection in apoptosis and autophagy, Biochim. Biophys. Acta 1813 (2011) 1003–1013, http://dx.doi.org/10.1016/j.bbamcr.2010.11.023.

[20] A. Espinosa, A. Garcia, S. Hartel, C. Hidalgo, E. Jaimovich, NADPH oxidase and hydrogen peroxide mediate insulin-induced calcium increase in skeletal

muscle cells, J. Biol. Chem. 284 (2009) 2568–2575, http://dx.doi.org/10.1074/jbc.M804249200.
[21] K. Kokame, K.L. Agarwala, H. Kato, T. Miyata, Herp, a new ubiquitin-like membrane protein induced by endoplasmic reticulum stress, J. Biol. Chem. 275 (2000) 32846–32853, http://dx.doi.org/10.1074/jbc.M002063200.
[22] Y. Okuda-Shimizu, L.M. Hendershot, Characterization of an ERAD pathway for nonglycosylated BiP substrates, which require Herp, Mol. Cell 28 (2007) 544–554, http://dx.doi.org/10.1016/j.molcel.2007.09.012.
[23] A. Schulze, S. Standera, E. Buerger, M. Kikkert, S. van Voorden, E. Wiertz, F. Koning, P.M. Kloetzel, M. Seeger, The ubiquitin-domain protein HERP forms a complex with components of the endoplasmic reticulum associated degradation pathway, J. Mol. Biol. 354 (2005) 1021–1027, http://dx.doi.org/10.1016/j.jmb.2005.10.020.
[24] S.L. Chan, W. Fu, P. Zhang, A. Cheng, J. Lee, K. Kokame, M.P. Mattson, Herp stabilizes neuronal Ca^{2+} homeostasis and mitochondrial function during endoplasmic reticulum stress, J. Biol. Chem. 279 (2004) 28733–28743, http://dx.doi.org/10.1074/jbc.M404272200.
[25] O. Hori, F. Ichinoda, A. Yamaguchi, T. Tamatani, M. Taniguchi, Y. Koyama, T. Katayama, M. Tohyama, D.M. Stern, K. Ozawa, Y. Kitao, S. Ogawa, Role of Herp in the endoplasmic reticulum stress response, Genes Cells 9 (2004) 457–469, http://dx.doi.org/10.1111/j.1356-9597.2004.00735.x.
[26] L. Yan, W. Liu, H. Zhang, C. Liu, Y. Shang, Y. Ye, X. Zhang, W. Li, Ube2g2-gp78-mediated HERP polyubiquitylation is involved in ER stress recovery, J. Cell Sci. 127 (2014) 1417–1427, http://dx.doi.org/10.1242/jcs.135293.
[27] C. Quiroga, D. Gatica, F. Paredes, R. Bravo, R. Troncoso, Z. Pedrozo, A. E. Rodriguez, B. Toro, M. Chiong, J.M. Vicencio, C. Hetz, S. Lavandero, Herp depletion protects from protein aggregation by up-regulating autophagy, Biochim. Biophys. Acta 1833 (2013) 3295–3305, http://dx.doi.org/10.1016/j.bbamcr.2013.09.006.
[28] C. Belal, N.J. Ameli, A. El Kommos, S. Bezalel, A.M. Al'Khafaji, M.R. Mughal, M. P. Mattson, G.A. Kyriazis, B. Tyrberg, S.L. Chan, The homocysteine-inducible endoplasmic reticulum (ER) stress protein Herp counteracts mutant alpha-synuclein-induced ER stress via the homeostatic regulation of ER-resident calcium release channel proteins, Hum. Mol. Genet. 21 (2012) 963–977, http://dx.doi.org/10.1093/hmg/ddr502.
[29] S. Chigurupati, Z. Wei, C. Belal, M. Vandermey, G.A. Kyriazis, T.V. Arumugam, S. L. Chan, The homocysteine-inducible endoplasmic reticulum stress protein counteracts calcium store depletion and induction of CCAAT enhancer-binding protein homologous protein in a neurotoxin model of Parkinson disease, J. Biol. Chem. 284 (2009) 18323–18333, http://dx.doi.org/10.1074/jbc.M109.020891.
[30] E. Jaimovich, C. Mattei, J.L. Liberona, C. Cardenas, M. Estrada, J. Barbier, C. Debitus, D. Laurent, J. Molgo, B. Xestospongin, a competitive inhibitor of IP3-mediated Ca^{2+} signalling in cultured rat myotubes, isolated myonuclei, and neuroblastoma (NG108-15) cells, FEBS Lett. 579 (2005) 2051–2057, http://dx.doi.org/10.1016/j.febslet.2005.02.053.
[31] Y. Zhang, K.K. Griendling, A. Dikalova, G.K. Owens, W.R. Taylor, Vascular hypertrophy in angiotensin II-induced hypertension is mediated by vascular smooth muscle cell-derived H_2O_2, Hypertension 46 (2005) 732–737, http://dx.doi.org/10.1161/01.HYP.0000182660.74266.6d.
[32] A. Criollo, L. Galluzzi, M.C. Maiuri, E. Tasdemir, S. Lavandero, G. Kroemer, Mitochondrial control of cell death induced by hyperosmotic stress, Apoptosis 12 (2007) 3–18, http://dx.doi.org/10.1007/s10495-006-0328-x.
[33] P. Marambio, B. Toro, C. Sanhueza, R. Troncoso, V. Parra, H. Verdejo, L. Garcia, C. Quiroga, D. Munafo, J. Diaz-Elizondo, R. Bravo, M.J. Gonzalez, G. Diaz-Araya, Z. Pedrozo, M. Chiong, M.I. Colombo, S. Lavandero, Glucose deprivation causes oxidative stress and stimulates aggresome formation and autophagy in cultured cardiac myocytes, Biochim. Biophys. Acta 1802 (2010) 509–518, http://dx.doi.org/10.1016/j.bbadis.2010.02.002.
[34] T. Gutierrez, V. Parra, R. Troncoso, C. Pennanen, A. Contreras-Ferrat, C. Vasquez-Trincado, P.E. Morales, C. Lopez-Crisosto, C. Sotomayor-Flores, M. Chiong, B.A. Rothermel, S. Lavandero, Alteration in mitochondrial Ca^{2+} uptake disrupts insulin signaling in hypertrophic cardiomyocytes, Cell Commun. Signal. 12 (2014) 68, http://dx.doi.org/10.1186/PREACCEPT-1950166084128344.
[35] R. Troncoso, F. Paredes, V. Parra, D. Gatica, C. Vasquez-Trincado, C. Quiroga, R. Bravo-Sagua, C. Lopez-Crisosto, A.E. Rodriguez, A.P. Oyarzun, G. Kroemer, S. Lavandero, Dexamethasone-induced autophagy mediates muscle atrophy through mitochondrial clearance, Cell Cycle 13 (2014) 2281–2295, http://dx.doi.org/10.4161/cc.29272.
[36] R. Troncoso, J.M. Vicencio, V. Parra, A. Nemchenko, Y. Kawashima, A. Del Campo, B. Toro, P.K. Battiprolu, P. Aranguiz, M. Chiong, S. Yakar, T.G. Gillette, J. A. Hill, E.D. Abel, D. Leroith, S. Lavandero, Energy-preserving effects of IGF-1 antagonize starvation-induced cardiac autophagy, Cardiovasc. Res. 93 (2012) 320–329, http://dx.doi.org/10.1093/cvr/cvr321.
[37] U. Weyemi, O. Lagente-Chevallier, M. Boufraqech, F. Prenois, F. Courtin, B. Caillou, M. Talbot, M. Dardalhon, A. Al Ghuzlan, J.M. Bidart, M. Schlumberger, C. Dupuy, ROS-generating NADPH oxidase NOX4 is a critical mediator in oncogenic H-Ras-induced DNA damage and subsequent senescence, Oncogene 31 (2012) 1117–1129, http://dx.doi.org/10.1038/onc.2011.327.
[38] V. Parra, V. Eisner, M. Chiong, A. Criollo, F. Moraga, A. Garcia, S. Hartel, E. Jaimovich, A. Zorzano, C. Hidalgo, S. Lavandero, Changes in mitochondrial dynamics during ceramide-induced cardiomyocyte early apoptosis, Cardiovasc. Res. 77 (2008) 387–397, http://dx.doi.org/10.1093/cvr/cvm029.
[39] V. Parra, F. Moraga, J. Kuzmicic, C. Lopez-Crisosto, R. Troncoso, N. Torrealba, A. Criollo, J. Diaz-Elizondo, B.A. Rothermel, A.F. Quest, S. Lavandero, Calcium and mitochondrial metabolism in ceramide-induced cardiomyocyte death, Biochim. Biophys. Acta 1832 (2013) 1334–1344, http://dx.doi.org/10.1016/j.bbadis.2013.04.009.
[40] C.Y. Jao, A. Salic, Exploring RNA transcription and turnover in vivo by using click chemistry, Proc. Natl. Acad. Sci. USA 105 (2008) 15779–15784, http://dx.doi.org/10.1073/pnas.0808480105.
[41] J. Chaudhuri, A.A. Chowdhury, N. Biswas, A. Manna, S. Chatterjee, T. Mukherjee, U. Chaudhuri, P. Jaisankar, S. Bandyopadhyay, Superoxide activates mTOR-eIF4E-Bax route to induce enhanced apoptosis in leukemic cells, Apoptosis 19 (2014) 135–148, http://dx.doi.org/10.1007/s10495-013-0904-9.
[42] K. Matsuno, H. Yamada, K. Iwata, D. Jin, M. Katsuyama, M. Matsuki, S. Takai, K. Yamanishi, M. Miyazaki, H. Matsubara, C. Yabe-Nishimura, Nox1 is involved in angiotensin II-mediated hypertension: a study in Nox1-deficient mice, Circulation 112 (2005) 2677–2685, http://dx.doi.org/10.1161/CIRCULATIONAHA.105.573709.
[43] J. Castro, C.X. Bittner, A. Humeres, V.P. Montecinos, J.C. Vera, L.F. Barros, A cytosolic source of calcium unveiled by hydrogen peroxide with relevance for epithelial cell death, Cell Death Differ. 11 (2004) 468–478, http://dx.doi.org/10.1038/sj.cdd.4401372.
[44] C. Brenner, M. Moulin, Physiological roles of the permeability transition pore, Circ. Res. 111 (2012) 1237–1247, http://dx.doi.org/10.1161/CIRCRESAHA.112.265942.
[45] A. Vianello, V. Casolo, E. Petrussa, C. Peresson, S. Patui, A. Bertolini, S. Passamonti, E. Braidot, M. Zancani, The mitochondrial permeability transition pore (PTP)-an example of multiple molecular exaptation? Biochim. Biophys. Acta 1817 (2012) 2072–2086, http://dx.doi.org/10.1016/j.bbabio.2012.06.620.
[46] M. Kny, S. Standera, R. Hartmann-Petersen, P.M. Kloetzel, M. Seeger, Herp regulates Hrd1-mediated ubiquitylation in a ubiquitin-like domain-dependent manner, J. Biol. Chem. 286 (2011) 5151–5156, http://dx.doi.org/10.1074/jbc.M110.134551.
[47] T. Marutani, T. Maeda, C. Tanabe, K. Zou, W. Araki, K. Kokame, M. Michikawa, H. Komano, ER-stress-inducible Herp, facilitates the degradation of immature nicastrin, Biochim. Biophys. Acta 1810 (2011) 790–798, http://dx.doi.org/10.1016/j.bbagen.2011.04.017.
[48] T. van Laar, T. Schouten, E. Hoogervorst, M. van Eck, A.J. van der Eb, C. Terleth, The novel MMS-inducible gene Mif1/KIAA0025 is a target of the unfolded protein response pathway, FEBS Lett. 469 (2000) 123–131.
[49] V. Eisner, A. Criollo, C. Quiroga, C. Olea-Azar, J.F. Santibanez, R. Troncoso, M. Chiong, G. Diaz-Araya, R. Foncea, S. Lavandero, Hyperosmotic stress-dependent NFkappaB activation is regulated by reactive oxygen species and IGF-1 in cultured cardiomyocytes, FEBS Lett. 580 (2006) 4495–4500, http://dx.doi.org/10.1016/j.febslet.2006.07.029.
[50] K.M. Spitler, R.C. Webb, Endoplasmic reticulum stress contributes to aortic stiffening via proapoptotic and fibrotic signaling mechanisms, Hypertension 63 (2014) e40–e45, http://dx.doi.org/10.1161/HYPERTENSIONAHA.113.02558.